Environment International 162 (2022) 107148

Contents lists available at ScienceDirect

Environment International

journal homepage: www.elsevier.com/locate/envint

Thallium isotopic compositions as tracers in environmental studies: A review

Qiaohui Zhong [a], Jianying Qi [b], Juan Liu [a,*], Jin Wang [a,g], Ke Lin [c], Qi'en Ouyang [a], Xian Zhang [a], Xudong Wei [a], Tangfu Xiao [a,h], Ali El-Naggar [d,e], Jörg Rinklebe [f]

[a] Key Laboratory of Water Quality and Conservation in the Pearl River Delta, Ministry of Education, School of Environmental Science and Engineering, Guangzhou University, Guangzhou, China
[b] South China Institute of Environmental Sciences, Ministry of Ecology and Environment, China
[c] Nanyang Technological University, Singapore 639798, Singapore
[d] University of Alberta, Edmonton, Alberta T6G 2E3, Canada
[e] Ain Shams University, Cairo 11241, Egypt, Department of Soil Sciences Faculty of Agriculture
[f] University of Wuppertal, School of Architecture and Civil Engineering, Institute of Foundation Engineering, Water- and Waste-Management, Laboratory of Soil- and Groundwater-Management, Pauluskirchstraße 7, 42285 Wuppertal, Germany
[g] Guangdong Provincial Key Laboratory of Radionuclides Pollution Control and Resources, Guangzhou, China
[h] State Key Laboratory of Geohazard Prevention and Geoenvironment Protection, Chengdu University of Technology, Chengdu, China

ARTICLE INFO

Keywords:
Thallium isotopes
Environmental contamination
Isotopic fractionation
Source tracer

ABSTRACT

Thallium is a highly poisonous heavy metal. Since Tl pollution control has been neglected worldwide until the present, countless Tl pollutants have been discharged into the environment, endangering the safety of drinking water, farmland soil, and food chain, and eventually posing a great threat to human health. However, the source, occurrence, pathway and fate of Tl in the environment remains understudied. As Tl in non-contaminated systems and from anthropogenic origin exhibits generally different isotopic signatures, which can provide fingerprint information and a novel way for tracing the anthropogenic Tl sources and understanding the environmental processes. This review summarizes: (i) the state-of-the-art development in highly-precise determination analytical method of Tl isotopic compositions, (ii) Tl isotopic fractionation induced by the low-temperature surface biogeochemical process, (iii) Tl isotopic signature of pollutants derived from anthropogenic activities and isotopic fractionation mechanism of Tl related to the high-temperature industrial activities, and (iv) application of Tl isotopic composition as a new tracer emerging tracer for source apportionment of Tl pollution. Finally, the limitations and possible future research about Tl isotopic application in environmental contamination is also proposed: (1) Tl fractionation mechanism in different environmental geochemistry processes and industrial activities should be further probed comprehensively; (2) Tl isotopes for source apportionment should be further applied in other different high Tl-contaminated scenarios (e.g., agricultural systems, water/sediment, and atmosphere).

1. Introduction

Elevated concentrations of toxic metal(loid)s arising from anthropogenic activities, threatening the quality of ecosystem and health of living beings, always draw considerable attention (Hou et al., 2020; Xiao et al., 2021; Yin et al., 2019). Thallium (Tl) is an exceedingly acute and non-essential element for all organisms, including humans (Rickwood et al. 2015; Voegelin et al., 2015; Wang et al., 2020; Genchi et al., 2021), and a Tl lethal dose for an adult human is only 8–10 mg/kg (Genchi et al., 2021; Wang et al., 2021; Wei et al., 2020). Tl primarily exists as Tl (I), whereas Tl(III) merely occurs in extreme oxidation and acidic environment (Karbowska, 2016; Wick et al., 2020). The extreme toxicity of Tl-based compounds is primarily induced by the high similarity between Tl(I) and K(I) ions that lead to the disorder of K(I) associated metabolic processes due to Tl interference (Wojtkowiak et al. 2016; Maya-Lo Pez et al., 2018; Zhang and Rickaby, 2020). It can induce gastrointestinal disease, dysfunction, nervous system disorder, nervous system, vital organs (e.g., kidneys, livers) damage, internal bleeding

* Corresponding author.
E-mail address: liujuan858585@163.com (J. Liu).

https://doi.org/10.1016/j.envint.2022.107148
Received 4 January 2022; Received in revised form 31 January 2022; Accepted 10 February 2022
Available online 24 February 2022

symptoms, and even death (Genchi et al., 2021; Osorio-Rico et al., 2017; Wang et al., 2020; Viraraghavan and Srinivasan, 2011). Hitherto, many countries (e.g., China, Russia, Australia, Europe and USA) have already listed Tl as a priority pollutant for control (USEPA, 2014; Coup and Swedlund, 2015; Cobelo-García et al., 2015; Belzile and Chen, 2017).

The natural abundance of Tl is generally low (She et al., 2022), but it can be enriched in various types of sulfide minerals, coal and K-silicate rocks, owing to its peculiar properties of both chalcophile and lithophile (Rader et al., 2018; Liu et al., 2019; Zhuang et al., 2021). Although the intended Tl global production only approximates 10 t/y, which is utilized in many different industrial manufacturing such as antifriction alloys, low-freezing alloys, photocells, low-melting special glasses, high-temperature superconductor materials and low-temperature thermometers (Karbowska 2016; Belzile and Chen 2017; Migaszewski and Gałuszka, 2021) and also utilized in medical area such as cardiovascular imaging for heart diseases and different cancer detections (USGS, 2019; Migaszewski and Gałuszka, 2021). However, Tl is released into the environment at 2000–5000 t/y as a by-product through various anthropogenic processes, such as Tl-rich sulfide ore/coal mining and other industrial activities using Tl-bearing minerals (e.g., metal smelting, sulfuric acid production, coal combustion, cement manufacturing) (Liu et al., 2020; Wang et al., 2020; Yin et al., 2021; Zhou et al., 2020; Wang et al., 2022), waste incineration, photocells, and antifriction alloys (Liu et al., 2016; Caritat and Reimann 2017; D'Orazio et al., 2020; Jiang et al., 2021).

Pertinent studies have investigated Tl distribution, enrichment, and environmental risks in different specific sites/areas during the last several decades (e.g., Liu et al., 2019; Rinklebe et al., 2020; Zhuang et al., 2021; Migaszewski and Gałuszka, 2021; Genchi et al., 2021). Even though Tl is considered as more poisonous to humans relative to Pb, Cd, Hg, Cu and Zn (Sinicropi et al., 2010; Carocci et al., 2014; Genchi et al., 2021). But the source, occurrence, pathway and fate of Tl, critical for Tl pollution control and prevention, remains largely unknown, when compared with other metals (e.g., Pb, Cd, Hg, Cu and Zn) well-studied. Traditionally statistical methods such as principal component analysis, cluster analysis, enrichment factors and geo-accumulation index cannot clearly speculate detailed source and quantify the contributions from every contamination source (Sun et al., 2018; Mirza et al., 2019). Isotopic fingerprint information offers precise proxies that can be employed to identify the contamination sources of heavy metals (Liu et al., 2020; Wang et al., 2021; Wei et al., 2020; Weiss et al., 2008; Wiederhold, 2015; Zeng and Han, 2020) or other types of pollutants (Liu and Han, 2021; Samantaray and Sanyal, 2022; Shen et al., 2021; Xiao et al., 2022). It has been demonstrated that Tl isotopic compositions can be utilized to determine the source apportionment and environmental processes (e.g., Kersten et al., 2014; Liu et al., 2022; Vaněk et al., 2016, 2021; Vejvodová et al., 2020). For examples, contaminated soil and sediment have recorded the Tl isotopic signature of Tl emissions from industrial pollutants near cement plant, Zn/Pb-smelter or coal-fired power plant, which evidently exhibited different Tl isotopic composition, as compared to natural background, providing fingerprint information for source tracing (Kersten et al., 2014; Vanek et al., 2016; 2018; Vanek et al., 2021; Liu et al., 2022).

This review herein summarizes the state-of-the-art development in (1) highly-precise determination analytical method of Tl isotopic compositions, (2) Tl isotopic fractionation induced by surface biogeochemical process, (3) Tl isotopic signature of pollutants derived from anthropogenic activities and (4) application of Tl isotopic compositions as a new emerging tracer for source apportionment of Tl pollution.

2. Tl isotopic analysis

2.1. Chromatographic separation

It is necessary to purify Tl from the various samples with complex matrix for high-precise Tl isotopic measurements (Rehkämper and Halliday, 1999; Nielsen et al. 2004, 2017a,b; Baker et al., 2009). A two-column separation procedure with AG1-X8 (200–400 mesh) resin was for the first time established for Tl isotopic determination from geological materials by Rehkämper and Halliday (1999). The first column was used to remove the most matrix, while Tl was further purified and reduced the residual sulfuric acid present by a second column. The key for this procedure is that Tl(III) generates strong anionic complexes with the halogens (either Cl^- or Br^-) and has a strong distribution capacity in AG1-X8 resin, while Tl(I) does not chelate with the halogens (either Cl^- or Br^-) and has very low distribution capacity in AG1-X8 resin (Nielsen et al., 2011, 2017a,b). Overall, there are three important steps for separation of Tl: 1) ensuring the complete conversion of all Tl(I) into Tl(III) before loading samples, 2) maintaining Tl(III) valence in the resin bed during eluting the matrix, and 3) converting Tl(III) into Tl (I) valence while collecting the Tl fraction. Based on the two-step chromatography developed by Rehkämper and Halliday. (1999), some steps were adjusted slightly for separating Tl from water samples by Nielsen et al. (2004) and for separating Tl and Cd from geological materials simultaneously by Baker et al. (2009). These optimized procedures can overall remove the matrix elements.

Taken all together, to avoid isotopic fractionation and matrix effect in instrumental measurement, Tl needs to be completely separated from the matrix elements with ~100% yield during the ion-exchange chemistry procedure (Rehkämper and Halliday, 1999; Nielsen et al. 2004; Baker et al. 2009). These separation methods can separate enough pure Tl for the accurate and precise analysis of Tl isotopic data. However, the whole separation procedure is time-consuming, which requires several types of acid (e.g., HCl, HBr, and HNO_3) and consumes large elution volumes. Thus, a more efficient and environment-friendly Tl chemical separation procedure needs to be developed in the near future.

2.2. Mass spectrometry

Thallium has two natural isotopes (^{203}Tl and ^{205}Tl) (Rehkämper and Nielsen, 2004). Tl isotopes was first measured in Thermal Ionization Mass Spectrometry (TIMS) with large instrumental mass bias, which made it difficult to distinguish the Tl isotopic fractionation between the standard and samples (Ostic et al., 1969). This limited the application of Tl stable isotope during past decades (Chen and Wasser-burg, 1994).

The first accurate determination of Tl isotopic compositions was achieved by Rehkämper and Halliday (1999), with the advent of Multi-Collector Inductively Coupled Plasma Mass Spectrometer (MC-ICP-MS) at the beginning of the 1990s (Walder and Freedman, 1992). They measured Tl isotopic compositions in different geological materials and meteorites, and the accuracy of Tl isotopic compositions reached 0.1–0.2‰, which was 3–4 times better than the best data measured by TIMS (Rehkämper and Halliday, 1999). The external accuracy was further improved to 0.1 during analyzing seawater and river samples with lower Tl contents (Nielsen et al., 2004). The precision of Tl isotopic determination for natural samples, instrument, instrumental mass bias and standard solution in different laboratories are summarized in **Table S1**. The precision of Tl isotopic determination for natural samples and Aldrich Tl solution are generally better than 0.09 and 0.08, respectively in the past decade (**Table S1**). Tl isotopic instrumental mass fractionation on MC-ICP-MS is generally corrected by the combination of standard sample bracketing and Pb external normalization, which can correct instrumental mass fractionation and instrumental drift simultaneously (Rehkämper and Halliday, 1999; Nielsen et al., 2012, 2017a,b; Baker et al., 2009). All laboratories adopt NIST SRM 997 Tl as the reference material ($\varepsilon^{205}Tl_{\text{NIST SRM 997}} = 0$) for Tl isotopes. Here, Tl isotopic data is expressed as follows:

$$\varepsilon^{205}Tl = \left[\left({}^{205}Tl/{}^{203}Tl \right)_{sample} / \left({}^{205}Tl/{}^{203}Tl \right)_{NISTSRM997} - -1 \right] \times 10^4 \quad (1)$$

Additionally, the ε^{205}Tl value of commonly used reference materials is compiled in **Table S2**. NOD-A-1 (Ferromanganese nodule) has the

heaviest ε^{205}Tl values with an average of 11.11 ± 0.29 (2SD, n = 18), which is related to the Tl(I) oxidative adsorption (Rehkämper et al., 2002; Rehkämper and Nielsen, 2004; Nielsen et al., 2013; Wick et al., 2019). While INCT-Tl-1 (Tea leaves) has the lightest ε^{205}Tl values with an average of −6.21 ± 0.90 (2SD, n = 6), likely indicating the preferential uptake of lighter Tl from soil (Vanek et al., 2019). All reference materials exhibit a total isotopic variability of larger than 17 ε^{205}Tl-units (**Table S2**), which may demonstrate the potential of Tl isotopic application in geo-environment. Reference materials including AGV-2 (-2.92 ± 0.43; 2SD, n = 57), BCR-2 (-2.4 ± 0.31; 2SD, n = 44), BHVO-2 (-1.58 ± 0.40; 2SD, n = 19), SCo-1 (-2.50 ± 0.33; 2SD, n = 2), 14P (-2.0 ± 0. 5; 2SD, n = 10), AL-I (-1.5 ± 0.2; 2SD, n = 5), AN-G (-2.7 ± 0.4; 2SD, n = 3), COQ-1 (-2.3 ± 0.5; 2SD, n = 5), GSP-2 (-2.5 ± 0.6; 2SD, n = 9), ISH-G (-1.5 ± 0.5; 2SD, n = 9), STM-1 (-2.0 ± 1.1; 2SD, n = 10) show similar Tl isotopic signature with bulk continental crust characterized by $\varepsilon^{205}Tl_{CONTCRUST}$ = -2.0 ± 1.0 (Anbar and Rouxel, 2007; Nilsen et al., 2005, 2017a,b).

3. Tl isotopic fractionation induced by the surface biogeochemical process

Metal isotopic fractionations potentially induced by post-release geological and biological processes (e.g., adsorption, complexation, interactions with plants) are called black-box isotope fractionation, which may alter the source information, thereby complicating isotope tracing (Komárek et al., 2021). Determining and understanding whether there is a Tl isotope fractionation black box or not is essential for isotope tracing in the environment. The magnitude of Tl isotopic fractionation in the various geo-environmental processes such as weathering, biological activities, adsorption and complexion processes may be different, and will be separately discussed according to previous experimental or natural investigation in the following.

3.1. Weathering process

Continental weathering process can lead to Tl migration and transfer in the environment, which may induce Tl isotopic fractionation. To evaluate whether there was Tl isotopic fractionation in weathering processes, waters, estuarine waters and suspended riverine particulates from different river were collected and analyzed (Nielsen et al., 2005). It was observed that dissolved riverine Tl ($\varepsilon^{205}Tl_{ave}$ = -2.5 ± 1) and particulate matter Tl ($\varepsilon^{205}Tl_{ave}$ = -2.0 ± 0.5) for many major/minor rivers exhibited identical Tl isotopic composition with continental crust ($\varepsilon^{205}Tl_{ave}$ = -2.0 ± 0.5), suggesting nil Tl isotopic fractionation during the weathering process. Howarth et al. (2018) revealed that weathering processes in red soil profiles can produce detectable Tl isotopic fractionation (1 ~ 2 ε^{205}Tl), likely due to Tl oxidative sorption and solution of mineralogy, where the highly reactive MnOs played the most important role (Wick et al., 2019; Nielsen et al., 2013). Additionally, the release of Tl from clay minerals may not cause Tl isotopic fractionation due to only occurrence of cation exchange without oxidation (Schauble, 2007; Martin et al., 2018; Wick et al., 2018, 2020). Negligible Tl isotopic fractionation may also occur during the weathering from sulfide minerals into pedogenic clay associated with only non-oxidative Tl(I) transfer (Vanek et al., 2020; Nielsen et al., 2017a,b; Schauble, 2007).

3.2. Biological activities

Biological activities also contribute to the transfer of Tl in the environment. Natural cabbages (ε^{205}Tl≈ −5.4– −2.5) were enriched in lighter Tl isotopes relative to its grown soil (ε^{205}Tl≈0.4), indicating preferential uptake of lighter ^{203}Tl from soil (Kersten et al., 2014). Analogously, Vanek et al. (2019) found that white mustard (ε^{205}Tl≈ −4.4– −3.0) were isotopically lighter than its hydroponic media (ε^{205}Tl≈ −2.7– −2.1), and white mustard growing with lower Tl concentration could produce a greater magnitude of Tl isotope fractionation. Additionally, in an Indian mustard-soil system, the early formed stems (ε^{205}Tl = 2.5) were systematically heavier than in plant parts formed later (e.g., leaves, flowers, seeds pods) (ε^{205}Tl = − 2.5 to + 0.1) (Rader et al., 2019). For these two experiments, white mustard grown in nutrient solutions and Indian mustard grown in soil both displayed regular plant-selective Tl isotopic fractionation behavior, in which lighter Tl was preferentially carried from soil/solution into roots, then stems and leaves, resulting in a depletion of Tl isotopic composition along the plant uptake paths (from roots to leaves) (**Figure S1**) (Vanek et al., 2019; Rader et al., 2019). These Tl isotopic fractionation behaviors (in white mustard and Indian mustard) may likely be some specific reactions (e.g., replacement of K(I) by Tl(I)), Tl transfers and Tl speciation (Rader et al., 2019; Vanek et al., 2019).

3.3. Tl adsorption and complexation

Due to bearing high and wide abundance, relative stability than other minerals, and high affinity of Tl(I), micaceous clay minerals such as illite and smectite are significant Tl adsorbent in soils and sediments (Wick et al., 2018, 2019; Martin et al., 2018). The adsorption of Tl(I) onto illite in different conditions can be described using a 3-site cation exchange model (Wick et al., 2018). Similarly, Martin et al. (2018) found that illite exhibited higher Tl affinity than smectite, and a multi-site ion exchanger model can be used to explain the adsorption behavior of Tl(I) onto illite and smectite. Additionally, only Tl(I) was found for adsorbed Tl onto illite and/or smectite by XANES spectra (Wick et al., 2018, 2020; Martin et al., 2018). Therefore, Tl(I) sorption onto clay minerals (e.g., illite and smectite) was propelled by exchange reactions and without oxidation of Tl(I) occurred, and no significant Tl isotopic fractionation was observed during these adsorption processes (Wick et al., 2018, 2020; Martin et al., 2018).

Manganese oxides (MnO_s) exhibit generally higher sorption capacity and affinity of Tl compared to the micaceous clay minerals, and both Tl (III) and Tl(I) sorption on MnO_s have been observed (Peacock and Moon, 2012; Nielsen et al., 2013; Wick et al., 2019). Pertinent studies have shown that only Tl(III) was found in hexagonal birnessite and δ-MnO_2 by oxidative adsorption of Tl(I), whereas Tl(I) was adsorbed on other types of MnO_s (e.g., HEPES-δ-MnO_2, Fe(II)-δ-MnO_2, triclinic birnessite, todorokite, cryptomelane) and ferrihydrite with Tl(I) adsorption directly (Bidoglio et al., 1993; Peacock and Moon, 2012; Wick et al., 2019). The adsorbed Tl on hexagonal birnessite was always isotopically heavier than aqueous Tl ($\varepsilon^{205}Tl_{solid\text{-}liquid}$ = 2.1–14.5) in different adsorption conditions (Nielsen et al., 2013, Fig. 1). A strong negative correlation (R^2 = 0.993) between contents of adsorbed Tl and magnitude of isotopic fractionation was also observed, possibly due to two diverse adsorption sites: (i) vacancy sites with isotopically fractionated Tl and (ii) unknown sorption sites with slightly fractionated Tl (Nielsen et al., 2013). The isotopic fractionation between Tl(I) and Tl(III) is largely ascribed to the nuclear volume effect of Tl, with the heavier ^{205}Tl isotope preferably enriched in Tl(III) (Schauble, 2007). The highly reactive MnO_s (e.g., hexagonal birnessite and δ-MnO_2) can oxidize most Tl(I) into Tl(III), followed by adsorbing them into vacancy sites with isotopically fractionated Tl in a certain range of Tl/Mn loading (Nielsen et al., 2013; Wick et al., 2019). However, with the increased loading of Tl/Mn, the oxidative Tl(III) uptake may be constrained by the enlarging of Mn reduction (Mn(IV) to Mn(III)) and declines in redox reactivity of MnO_s, resulting in a direct Tl(I) adsorption into remaining sites with no fractionated Tl (Wick et al., 2019).

As displayed in Fig. 2, Tl isotopes can also provide new insight into Tl biogeochemical cycle in the soil profile. For two natural Tl-rich soil profiles (Erzmatt, Swiss), Tl isotopic composition of bottom C horizons (ε^{205}Tl = 0.8–2.6) increased gradually to the uppermost Bw horizons (ε^{205}Tl = 8.7), then decreased to the overlying O horizons (ε^{205}Tl = 2.5) (Vanek et al., 2020). The isotopic shift in soil profiles may be related to cyclic Tl mobilization and immobilization processes throughout parental rock weathering and subsequent soil formation (Fig. 2).

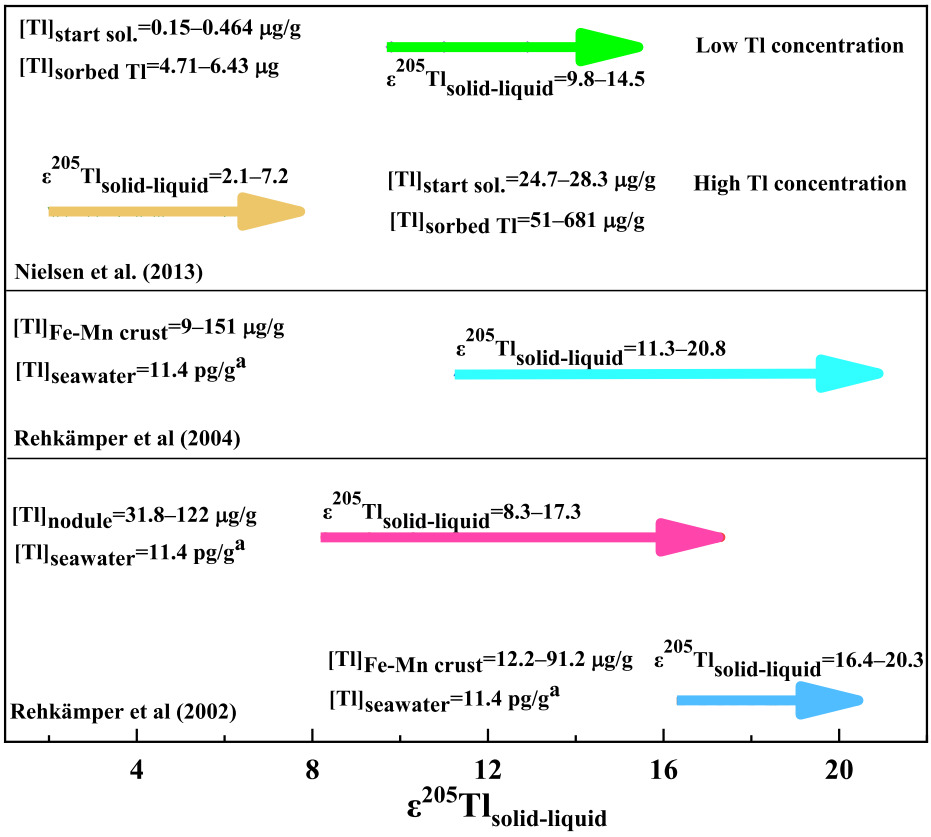

Fig. 1. Tl isotopic fractionation during the Tl adsorption onto Mn-oxides (experimental) and hydrogenetic Fe-Mn crust/nodule (natural). $\varepsilon^{205}Tl_{solid\text{-}liquid} = \varepsilon^{205}Tl_{solid} - \varepsilon^{205}Tl_{liquid}$; [a]The data of $[Tl]_{Seawater}$ = 11.4 pg/g and $\varepsilon^{205}Tl_{seawater}$ = -6 used for calculation of $\varepsilon^{205}Tl_{solid\text{-}liquid}$ of Fe-Mn crust/nodules are from Owens et al. (2017).

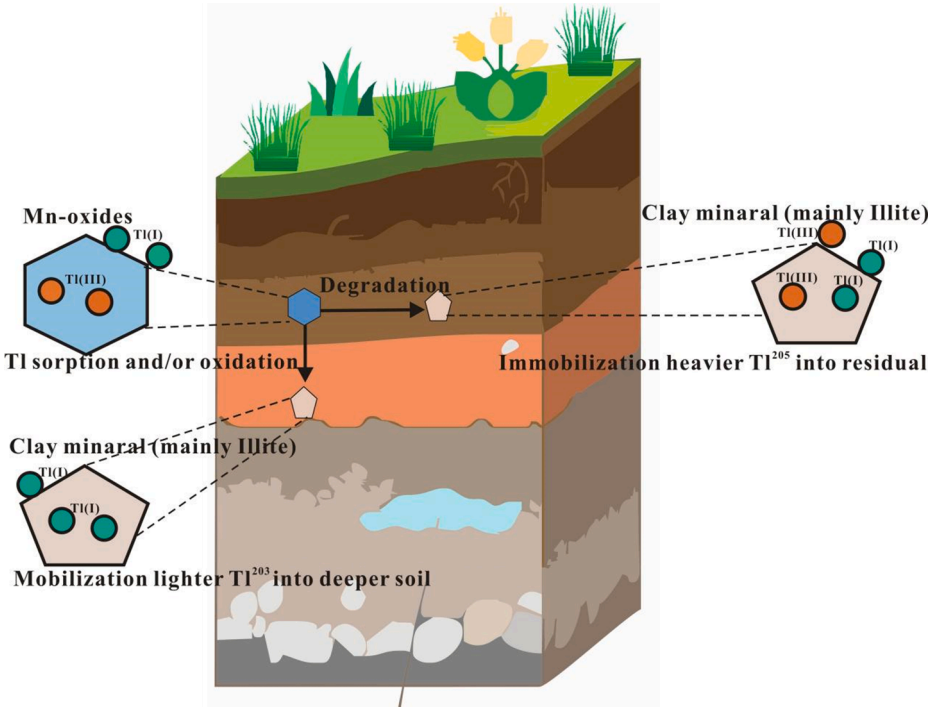

Fig. 2. Systematic (redox-driven) MnOs degradation and Tl cycling in the soil profile.

Transfer processes of Tl in soil profile may involve: (i) MnOs adsorb and oxidize Tl(I) into Tl(III), leading to the enrichment of heavier ^{205}Tl, and (ii) the Tl(III)-containing MnOs are weathered gradually, in which the isotopically lighter Tl(I) can mobilize into deeper horizons, and the isotopically heavier Tl(III) and/or partial Tl(I) can remobilize into other phases (mainly illite) related to subsequent soil formation (Fig. 2). Similarly, a good relationship (R^2 = 0.6) between the soil MnOs concentration (oxalate-extractable data) and Tl isotopic fractionation degree, and a peak Mn and/or Fe concentrations at the Ah/Bw horizon interface (oxalate-extractable data) can be found in a Tl-rich natural soil profile (Kluky, Czech Republic) (Vejvodová et al., 2020). In addition, the oxalate extract data (ε^{205}Tl = 14.4) or the total digested data (ε^{205}Tl = 8.17) for MnOs nodules sample exhibited an evident Tl isotopic fractionation compared with soil clay (ε^{205}Tl = 4.57) (Vejvodová et al., 2020). Similar to the Tl fractionation behaviour observed in Vanek et al. (2020), the Tl isotopic variation in this studied soil profile may also primarily be controlled by the oxidative Tl uptake of MnOs and then alteration of soil Tl-bearing MnOs induced by pedogenesis (Vejvodová et al., 2020; Fig. 2).

4. Tl isotopic signatures derived from anthropogenic activities

4.1. The ε^{205}Tl signatures of different metallic sulfide ores

Thallium isotopic signatures in metallic sulfide ores are summarized in Fig. 3. The ε^{205}Tl values of diagenetic pyrite deposited under oxic water and pyrite formed during oceanic anoxia ranged from −5.4 to 6.4 and −7.8 to 1.9, respectively (Nielsen et al., 2011). The ε^{205}Tl values of chalcopyrite from global localities was measured to be −1.0 ~ 17.8, while those of galena from Australia averaged at 4.4 ± 0.7 (Rader et al., 2018). Pyrite ore (for producing sulfuric acid) from Germany ($\varepsilon^{205}Tl_{pyrite}$ = -0.36 ± 0.55) and China ($\varepsilon^{205}Tl_{pyrite}$ = 1.28 ± 0.2), coal pyrite (for coal burning) from Czech Republic ($\varepsilon^{205}Tl_{pyrite}$ = -5.54 ± 0.7) exhibit remarked isotopic difference (Kersten et al., 2014; Vaněk et al., 2016; Liu et al., 2020). Zinc ore (-3.76 ± 0.7) and post-flotation Zn-Fe residue (-3.89 ± 0.7) from Zn smelter (Poland) exhibit similar ε^{205}Tl value, suggesting no Tl isotopic fractionation during ore flotation (Vaněk et al., 2018), while Pb-Zn ore (-1.0 ± 0.17) from Pb-Zn smelter (China) yielded a heavier ε^{205}Tl value (Zhou et al., 2021). Zinc ore (-4.20 ± 0.7) and post-flotation of mixed Pb-Zn ore (-4.40 ± 0.7) from Olkusz mine yielded identical Tl isotopic compositions (Vaněk et al., 2021). Post-flotation wastes of Pb-Zn ore from Namibia mine were in the range of 3.6–14.6 (Grosslova et al., 2018). Overall, raw sulfide minerals (e.g., Zn ore, pyrite) from various mines are characterized by different Tl isotopic signatures, most possibly owing to the formation and/or post-alteration of raw ore. Therefore, Tl-bearing pollutants from industries related to these raw materials can also exhibit various Tl isotopic signatures.

4.2. Tl isotopic fractionation in high-temperature industrial processes

High-temperature industrial activities that employed sulfide ores or coal as raw materials are significant sources of Tl for the environment. Owing to highly volatile properties, Tl and Tl compounds are easily evaporated into the vapor phase during high-temperature processes (Chen et al., 2013; Antón et al., 2013; Liu et al., 2020). Thus, a comprehensive evaluation of Tl isotopic fractionation in these industries is indispensable for source tracking of Tl contamination. Tl isotopic signatures of raw materials and waste materials from different high-temperature industrial activities are compiled in **Figure S2**.

In a coal-fired power plant, Prague, the bottom ash ($\varepsilon^{205}Tl_A$ = -0.16 ± 0.7, $\varepsilon^{205}Tl_B$ = 0.23 ± 0.7) of both energy sources (A and B zone) have heavier isotopic signature than fly ash ($\varepsilon^{205}Tl_A$ = -2.50 ± 0.7, $\varepsilon^{205}Tl_B$ = -2.82 ± 0.7) (**Figure S2**, Fig. 4**a**) (Vaněk et al., 2016). Approximately 83% of Tl were evaporated from coal pyrite into gaseous Tl, and the Tl volatile fractions exhibited isotopically lighter Tl (ε^{205}Tl = -10.3 ± 0.7 ~ -6.16 ± 0.7) than initial coal pyrite (ε^{205}Tl = -5.54 ± 0.7) (Vaněk et al., 2016). Slag, bottom ash, fly ash, and pyrite ore from the sulfuric acid factory also displayed similar Tl isotopic fractionation behavior (Liu et al., 2020). As showed in Fig. 4**b and Figure S2**, slag (ε^{205}Tl = 16.24

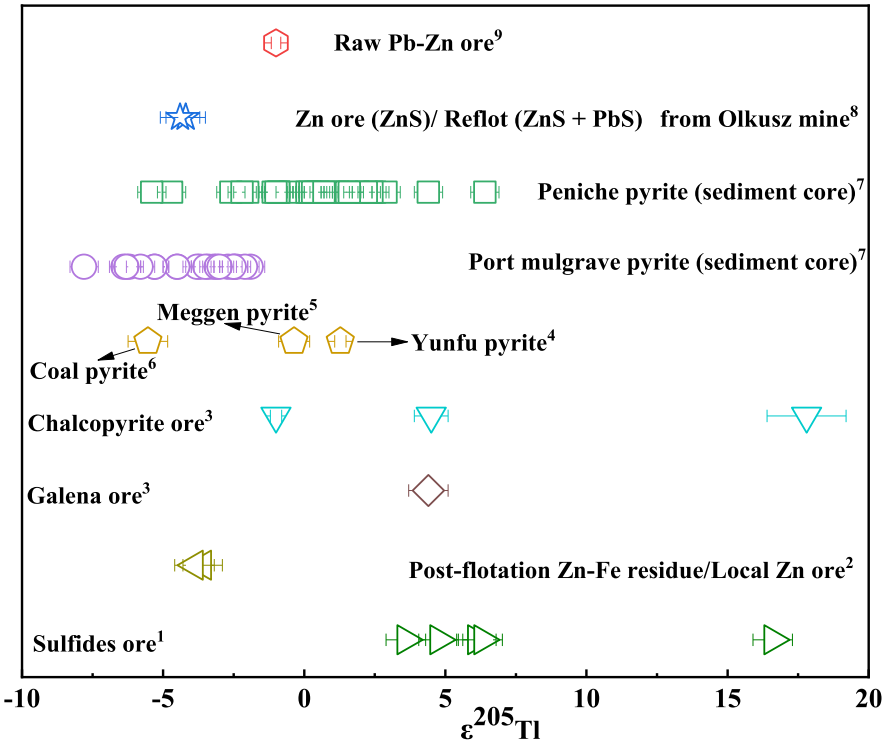

Fig. 3. Thallium isotopic compositions in different sulfide ores. Data are obtained from Grösslová et al. (2018)[1], Vaněk et al. (2018)[2], Rader et al. (2018)[3], Liu et al. (2020)[4], Kersten et al. (2014)[5], Vaněk et al. (2016)[6], Nielsen et al. (2011)[7], Vaněk et al. (2021)[8] and Zhou et al. (2021)[9].

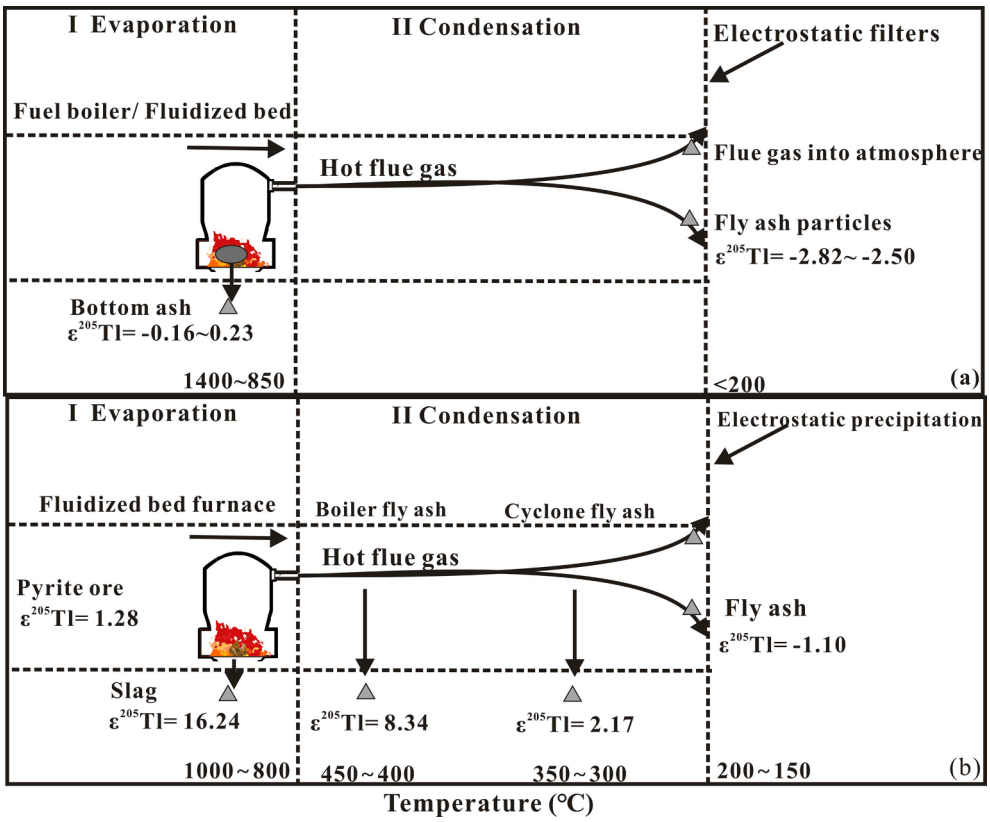

Fig. 4. Tl isotopic Fractionation during evaporation and condensation in industry, a) a coal-fired power plant; b) a sulfuric acid factory.

± 0.2, [Tl] = 28.0 ± 1.1 mg/kg) from fluidized-bed furnace and subsequent boiler fly ash (ε^{205}Tl = 8.34 ± 0.2, [Tl] = 36.9 ± 1.8 mg/kg), cyclone fly ash (ε^{205}Tl = 2.17 ± 0.2, [Tl] = 39.6 ± 1.6 mg/kg) and electrostatic precipitator fly ash (ε^{205}Tl = -1.10 ± 0.2, [Tl] = 75.0 ± 3.6 mg/kg) displayed a significant Tl isotopic fractionation.

Similarly, the slag (ε^{205}Tl = -3.3 ± 0.7), local Zn ore (ε^{205}Tl = -3.76 ± 0.7) and fly ash (ε^{205}Tl = -4.1 ± 0.7) from Boleslaw Zn smelter, Poland showed identical Tl isotopic fractionation pattern (**Figure S2**) (Vaněk et al., 2018, 2021). The final refinement waste exhibited the lowest ε^{205}Tl value (-4.77 ± 0.7), which may be impacted by the extraction of volatile lighter Tl and then co-precipitation with newly-formed (secondary) waste. Granulated waste generated from diverse stages of Zn hydrometallurgical processes was characterized by identical Tl isotopic signatures within the uncertainty of Zn ore. In addition, Tl isotopic fractionation behavior among clinker, electrostatic precipitator dust (ε^{205}Tl = -2.03 ± 0.14) and electrostatic precipitator dust (ε^{205}Tl = -2.03 ± 0.14) from a Pb-Zn smelter, China (Zhou et al., 2021) was similar to those in the Zn smelter (Vaněk et al., 2018, 2021). Obvious ^{205}Tl enrichment in clinker (produced in the blast furnace) was mainly induced by the volatilization of lighter Tl preferentially. Acid sludge (ε^{205}Tl = -4.62 ± 0.76) from the production of H_2SO_4 and lime neutralizing slag (ε^{205}Tl = -2.36 ± 0.18) from precipitation of dedusting wastewater both were featured by lighter Tl isotopic composition, which likely captured very light volatile Tl and then co-precipitated into sludge or neutralizing slag.

Tl isotopic fractionation in high-temperature industrial activities (e.g., coal combustion, Pb/Zn smelting, and pyrite smelting) mainly incorporate two processes: evaporation and condensation (Vaněk et al., 2016, 2018; Liu et al., 2020; Zhou et al., 2021). Similar metal isotopic fractionation patterns such as Cd and Zn isotopes are also observed, which are related to evaporation and condensation processes (e.g., Gonzalez and Weiss, 2015; Fouskas et al., 2018; Zhong et al., 2021). In the high-temperature furnace, the heavier Tl isotopes are retained in the solid residual (e.g., slag or bottom ash), while the lighter Tl isotopes can generally be evaporated into the volatile phase, which is mainly controlled by the evaporation process (Fig. 4). However, after flowing out of the furnace, the relative heavier Tl fractions from the flue gas condenses preferentially and re-adsorbs on the surface of dust/fly ash particles, subsequently by the further accumulation of Tl gradually during condensation processes (Fig. 4). This is likely because partial re-equilibrant reactions of the vapor phase Tl related to the condensation process have occurred due to a quick decrease in temperature. The Tl isotopic fractionation and evolution within these high-temperature processes can be approximately described by the Rayleigh fractionation model (*Eq.* (2)) within a closed system (Liu et al., 2020; Zhou et al., 2021).

$$\varepsilon^{205}\mathrm{Tl}_{\mathrm{volatile}} = \left[\left(10^4 + \varepsilon^{205}\mathrm{Tl}_{\mathrm{raw\ material}}\right) \times \frac{\left(1 - f^{(1/\alpha)}\right)}{(1 - f)}\right] \quad (2)$$

Where $\varepsilon^{205}\mathrm{Tl}_{\mathrm{volatile}}$ and $\varepsilon^{205}\mathrm{Tl}_{\mathrm{raw\ materials}}$ are Tl isotopic compositions of volatile and raw materials, respectively. α is Tl isotopic fractionation factor, and *f* is the mass fraction ratio of Tl in the residual.

In summary, the high-temperature industrial process can induce obvious Tl isotopic fractionation, in which isotopically lighter Tl is generally observed in the fly ash or vapor Tl fraction, whereas the heavier Tl is enriched in the residual slag or bottom ash (**Figure S2** and Fig. 4). The raw material from different sites (see section 4.1) can bring distinct Tl isotopic composition of those waste materials. Furthermore, the different actual operations and techniques in industrial activities may also cause various Tl isotopic fractionation among fly ash, slags, bottom ash, etc. in the industrial processes as shown in Cd isotopes (Cloquet et al., 2005; Zhong et al., 2020). Thus, Tl isotopic signatures of raw material and waste materials generated from various industrial processes generally exhibit its fingerprint information, which can be distinguished from geogenic sources in the environment and be employed as an environmental tracer to identify released Tl from the

different industrial sources.

5. Application of Tl isotopes as a tracer for environmental pollution

Prior to the utilization of Tl isotopes in tracing Tl sources in studied areas, the geo-environmental situation and/or industry should be first investigated, to predict the potential contamination sources and Tl geo-environmental migration behavior. Thereafter, adequate and representative environmental samples such as the contaminated samples, potential source materials and natural background samples for source identification should be carefully selected. By measuring Tl content of collected natural soil samples and investigating the natural parental bedrocks (i.e. local background) in the studied area, environmental evaluation methods such as enrichment factors, geo-accumulation index can be used to judge whether the selected natural soil samples are

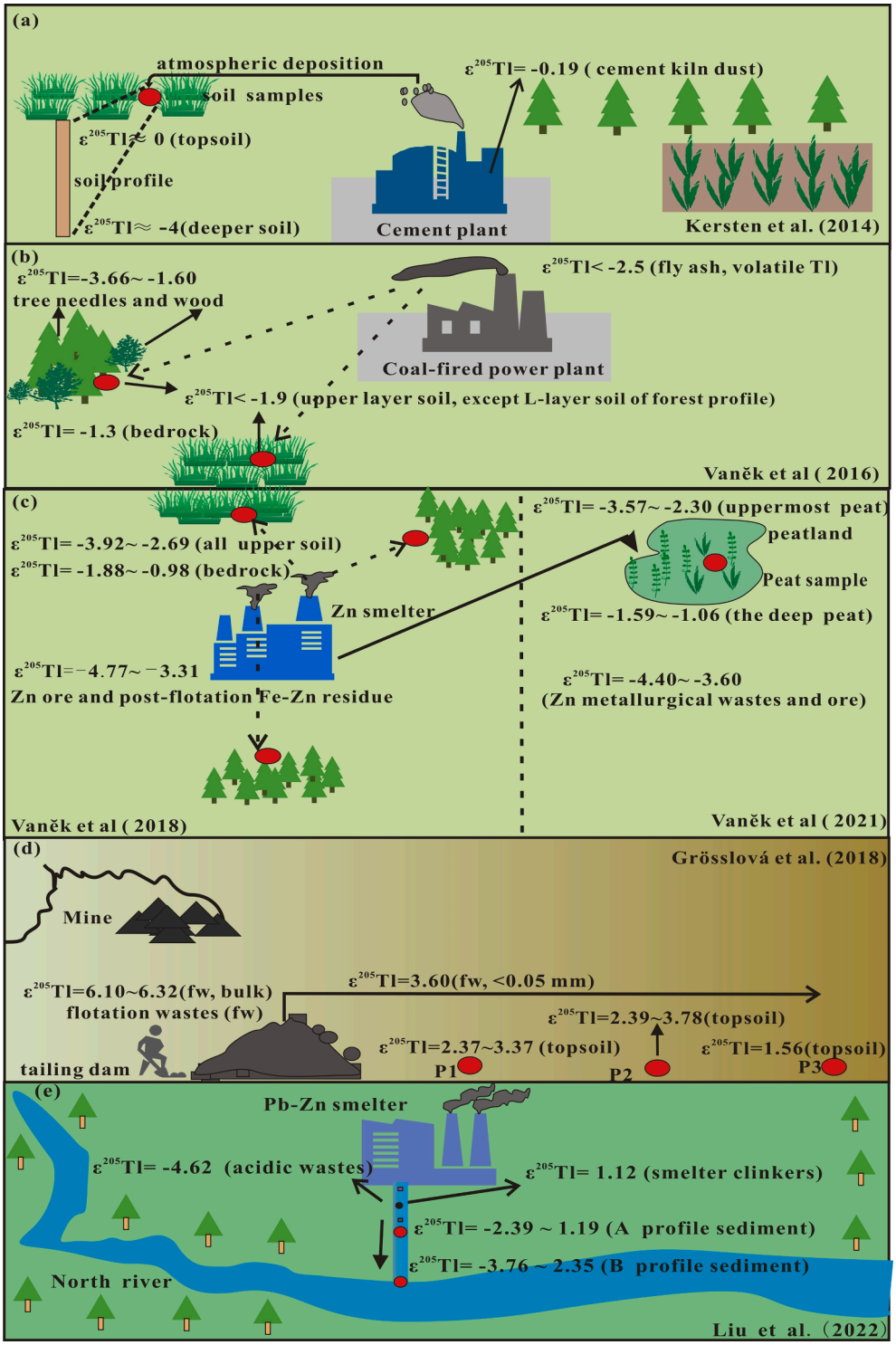

Fig. 5. Application of Tl isotopes in tracing Tl pollution in environment. a) tracing soil Tl contamination near a cement plant; b) tracing soil Tl contamination near a coal-fired power plant; c) tracing soil and peat Tl contamination near a Zn smelter; d) tracing soil Tl contamination near a mining site; e) tracing sediment Tl contamination near a Pb-Zn smelter.

suitable for natural background (Ahmed et al., 2018; Liu et al., 2017). The ideal case is that the studied samples are affected by only two sources (i.e., natural and anthropogenic sources) with significantly different Tl isotopic signatures. When there is a significant linear correlation between ε^{205}Tl values and 1/Tl of end-elements/mixed environmental samples, a simple binary mixed model (*Eq.* (3) and (4)) can be used to quantitatively estimate the contribution of each source to the environmental samples (Weiss et al., 2008; Wiederhold, 2015).

$$\varepsilon_M = \varepsilon_A \times f_A + \varepsilon_B \times f_B \quad (3)$$

$$f_A + f_B = 1 \quad (4)$$

Where ε_M is the isotopic value of the mixture, ε_A and ε_B is the isotopic value of the anthropogenic source and the natural source, while f_A and f_B are the contribution ratios of anthropogenic and natural sources, respectively.

Kersten et al. (2014) first utilized Tl isotopic compositions to track the sources of Tl input in soil profiles near the Lengerich cement plant, Germany. The results showed that deep background soils (ε^{205}Tl≈ −4) were isotopically lighter than topsoils (ε^{205}Tl≈0), which exhibited similar Tl isotopic composition as that of cement kiln dust (ε^{205}Tl = -0.19 ± 0.40) and Meggen pyrite (ε^{205}Tl = -0.36 ± 0.55) (a mix addition during cement production) (Kersten et al., 2014). A plot of ε^{205}Tl *vs.* 1/[Tl] indicated that the soils were contaminated by dust emissions from the Lengerich cement plant and background Tl (Fig. 5**a** and **Figure S3**). Forest and grassland soil profiles near coal-fired power plants, Czech Republic (Vaněk et al., 2016) and near Zn smelter, Poland (Vaněk et al., 2018) exhibited that the Tl-contaminated upper soils were enriched in lighter Tl isotopes relative to bedrock. In particular, Tl isotopic signatures of upper soils (ε^{205}Tl < -1.9) near coal-fired power plants were identical to fly ash and volatile Tl (ε^{205}Tl < -2.5) (Vaněk et al., 2016), while the Tl-contaminated upper soils (ε^{205}Tl = -3.92 – -2.69) near Zn smelter presented similar Tl isotopic composition to the waste materials Zn ore, post-flotation Zn-Fe residue (ε^{205}Tl = -4.77 – -3.31) (Vaněk et al., 2018). The diagram of ε^{205}Tl versus 1/[Tl] in both studies demonstrated a mixing of Tl input derived from both industrial sources (coal-fired power plants or Zn smelter) and geogenic source (Fig. 5**b, c** and **Figure S3**).

Mining activities also can generate evident Tl isotopic variations in soils. Both Tl-contaminated P1 and P2 soil profiles near an arid desert Pb-Zn ore mining, Namibia presented an evident enrichment of heavier Tl in the topsoils (ε^{205}Tl = 2.37–3.78) than the bottom soil (ε^{205}Tl = -0.38– 0.80) (Grösslová et al., 2018). At the same time, the soils in the most distant P3 profile exhibited low Tl accumulation and different isotopic variation. Additionally, the ε^{205}Tl values of topsoils were identical to < 0.05 mm fine particulate matter (ε^{205}Tl = 3.60) from mine tailings, indicating the Tl input of pollution. The diagram of ε^{205}Tl versus 1/[Tl] revealed a binary mixing of Tl impacted by mining-derived source (waste of Pb-Zn mine tailings, especially < 0.05 mm fine particle) and geogenic origin (Fig. 5**d** and **Figure S3**). The binary mixing model demonstrated that over one third of Tl contamination topsoil from the studied depth profiles was attributed to flotation waste-derived load.

However, the simple binary mixing model is not suitable for evaluating the source of Tl in complicated environmental settings with complex Tl pollution sources (e.g., mining activities, metal smelting, fertilizer use, coal combustion, transportation emissions, etc.). Therefore, the isotope multi-source mixing model is proposed by Liu et al. (2022):

$$\varepsilon_M = \varepsilon_1 \times f_1 + \varepsilon_2 \times f_2 + \cdots + \varepsilon_n \times f_n \quad (5)$$

$$f_1 + f_2 + \cdots + f_n = 1 \quad (6)$$

Where ε_M is the value of the mixture, ε_n is the Tl isotopic value of different end-members. *f*n is the Tl contribution ratio of different end-members. Isotopic multi-source hybrid models use the ISosource software to calculate the source of pollution and assess the contribution of each source. The ISosource program analyzes all possible combinations of the contribution rate of each potential source in a small mass balance tolerance (Chen et al., 2018; US EPA, 2017; Wang et al., 2021).

Two sediment profiles from downstream of a Pb-Zn smelter outfall yielded ε^{205}Tl values ranging from −3.76 to 2.35 (most sediments yielded ε^{205}Tl values = -3.76–1.01) that was found between acidic wastes (ε^{205}Tl = -4.62) and smelter clinkers (ε^{205}Tl = 1.12) (Liu et al., 2022). In the ε^{205}Tl vs 1/Tl diagram, the sediments did not align with a single line, which may suggest at least three various sources input with distinct Tl isotopic signatures, i.e., smelter clinkers, acidic wastes, and local background (Fig. 5**e** and **Figure S3**). The mixing model exhibited that ~ 80% of Tl pollution in sediments was caused by the smelter wastes. Moreover, the uppermost peat (ε^{205}Tl = -3.57 – -2.30) (0–14 cm) near Boleslaw Zn smelter was featured by similar isotopic signatures to local ore and/or Zn metallurgical wastes (ε^{205}Tl = -4.40 to −3.60) (Vaněk et al., 2021). In contrary, the deeper peat (34–40 cm) and clayey sand (120–150 cm, background) (ε^{205}Tl = -1.47) were characterized by identical Tl isotopic composition (ε^{205}Tl ≥ -1.59 ~ -1.06). They referred that the uppermost Tl-contaminated peat was likely induced by Tl emissions from near Zn smelter, whereas the deeper peat (≥34 cm) was influenced by geogenic Tl (Vaněk et al., 2021). Additionally, the ^{206}Pb/^{207}Pb ratios of upper peat (1.1722–1.1906) (0–40 cm) was analogous to those observed in local ore (1.173) and fly ash (1.174), indicating a great contribution of the Tl input from Zn smelter, whereas ^{206}Pb/^{207}Pb ratios of deeper peat (1.1641–1.1792) indicated a geogenic source (Vaněk et al., 2021). Altogether, ^{206}Pb/^{207}Pb ratios demonstrated a consistent result with Tl isotopic data, further supporting the potential employment of ε^{205}Tl values as proxies for Tl contamination source in sediment (Fig. 5**c** and **Figure S3**).

6. Conclusion and perspectives

The advent of MC-ICP-MS has improved precise measurement of Tl isotopic compositions, which offers a newly promising technique to understand Tl's geochemical cycle (e.g., source, occurrence, transfer and fate), providing important insight for source tracing of Tl contamination in the environment. The application of Tl isotopic compositions in environmental contamination is comprehensively summarized herein for the first time. Thallium isotopic fractionation induced by the surface naturally geochemical process is limited as compared to that by high-temperature industrial processes. The unique extensive Tl isotopic fractionation derived from industrial activities shows great potential for source apportionment of Tl pollution in environmental media using Tl isotopic signatures. However, as a relatively emerging field, there are still challenges in Tl isotopic application in the environment, which demonstrates that more studies are needed to broaden this field. For example, the "Tl isotope fractionation black box" is induced in the environment due to post-release geological and biological processes and should be carefully considered when deciphering the Tl isotopic results. Future research should focus on and further explore several aspects:

1) More studies on natural processes and/or experimental simulations are required to identify the Tl fractionation mechanism in different environmental geochemistry processes. Additionally, Tl isotopic fractionation in different anthropogenic activities such as metal ore/coal mining and processing, metal smelting and refining, coal/lignite combustion, waste incineration, petroleum refining, cement manufacturing processes should be further investigated comprehensively.
2) The application of Tl isotopes as the source tracer is mainly concentrated in soil and sediment contamination. However, compared with other well-studied metals isotopes (e.g., Pb, Cd, Cu, Zn and Hg), Tl isotopes in different environmental media for contamination sources remain obscure. It is time to investigate the source apportionment further using Tl isotopes in different high Tl-

contaminated environments, such as agricultural systems (soil-crop), water, sediment, aquatic organism and atmosphere.

3) Thallium isotopes have been widely utilized to investigate different Tl geochemistry (e.g., cosmos, mantle, paleocean), there are still many unexplored but potentially advantageous applications of Tl isotopes. For examples, Tl isotopes may also be applied to understand biological mediated fractionation of Tl isotopes and investigate the potential application of Tl isotopes in climate change research.

Declaration of Competing Interest

The authors declare that they have no known competing financial interests or personal relationships that could have appeared to influence the work reported in this paper.

Acknowledgment

This work was supported by the National Natural Science Foundation of China (Nos. 42173007; 41873015; 41830753) and the Guangdong Provincial Natural Science Foundation (2021B1515020078; 2021A1515011588).

Appendix A. Supplementary data

Supplementary data to this article can be found online at https://doi.org/10.1016/j.envint.2022.107148.

References

Ahmed, I., Mostefa, B., Bernard, A., Olivier, R., 2018. Levels and ecological risk assessment of heavy metals in surface sediments of fishing grounds along Algerian coast. Mar. Pollut. Bull. 136, 322–333.

Antón, M.A.L., Spears, D.A., Somoano, M.D., Tarazona, M.R.M., 2013. Thallium in coal: analysis and environmental implications. Fuel, 105, 13–18.

Anbar, A.D., Rouxel, O., 2007. Metal stable isotopes in paleoceanography. Ann. Rev. Earth Planet. Sci. 35 (1), 717–746.

Baker, R.G.A., Rehkämper, M., Hinkley, T.K., Nielsen, S.G., Toutain, J.P., 2009. Investigation of thallium fluxes from subaerial volcanism-Implications for the present and past mass balance of thallium in the oceans. Geochim. Cosmochim. Acta 73 (20), 6340–6359.

Belzile, N., Chen, Y.-W., 2017. Thallium in the environment: a critical review focused on natural waters, soils, sediments and airborne particles. Appl. Geochem. 84, 218–243.

Bidoglio, G., Gibson, P.N., O'Gorman, M., Roberts, K.J., 1993. X-ray-absorption spectroscopy investigation of surface redox transformations of thallium and chromium on colloidal mineral oxides. Geochim. Cosmochim. Acta 57 (10), 2389–2394.

de Caritat, P., Reimann, C., 2017. Publicly available datasets on thallium (Tl) in the environment–a comment on Presence of thallium in the environment: sources of contaminations, distribution and monitoring methods by Bozena Karbowska. Environ. Monit. Assess. 188, 640.

Carocci, A., Rovito, N., Sinicropi, M.S., Genchi, G., 2014. Mercury toxicity and neurodegenerative effects. Rev. Environ. Contaminat. Toxicol. 229, 1–18.

Chen, J.H., Wasserburg, G.J., 1994. The abundance of thallium and premordial lead in selected meteorites–the search for ^{205}Pb. LPSC XXV 245–246.

Chen, YongHeng, Wang, ChunLin, Liu, J., Wang, J., Qi, JianYing, Wu, YingJuan, 2013. Environmental exposure and flux of thallium by industrial activities utilizing thallium-bearing pyrite. Sci. China Earth Sci. 56 (9), 1502–1509.

Chen, L., Zhou, S., Wu, S., Wang, C., Li, B., Li, Y., Wang, J., 2018. Combining emission inventory and isotope ratio analyses for quantitative source apportionment of heavy metals in agricultural soil. Chemosphere 204, 140–147.

Cloquet, C., Carignan, J., Libourel, G., 2005. Kinetic isotopic fractionation of Cd and Zn during condensation. American Geophysical Union, Fall Meeting 2005.

Cobelo-García, A., Filella, M., Croot, P., Frazzoli, C., Du Laing, G., Ospina-Alvarez, N., Rauch, S., Salaun, P., Schäfer, J., Zimmermann, S., 2015. COST action TD1407: network on technology-critical elements (NOTICE)–from environmental processes to human health threats. Environ. Sci. Pollut. Res. 22, 15188–15194.

Coup, K.M., Swedlund, P.J., 2015. Demystifying the interfacial aquatic geochemistry of thallium(I): New and old data reveal just a regular cation. Chem. Geol. 398, 97–103.

D'Orazio, M., Campanella, B., Bramanti, E., Ghezzi, L., Onor, M., Vianello, G., Vittori-Antisari, L., Petrini, R., 2020. Thallium pollution in water, soils and plants from a past-mining site of Tuscany: sources, transfer processes and toxicity. J. Geochem. Explor. 209, 106434. https://doi.org/10.1016/j.gexplo.2019.106434.

Fouskas, F., Ma, L., Engle, M.A., Ruppert, L., Geboy, N.J., Costa, M.A., 2018. Cadmium isotope fractionation during coal combustion: Insights from two US coal-fired power plants. Appl. Geochem. 96, 100–112.

Genchi, G., Carocci, A., Catalano, L., Sinicropi, M.S., Catalano, A., 2021. Thallium use, toxicity, and detoxification therapy: an overview. Appl. Sci. 2021 (11), 8322.

Grösslová, Z., Vaněk, A., Oborná, V., Mihaljevič, M., Ettler, V., Trubač, J., Drahota, P., Penížek, V., Pavlů, L., Sracek, O., Kříbek, B., Voegelin, A., Göttlicher, J., Drábek, O., Tejnecký, V., Houška, J., Mapani, B., Zádorová, T., 2018. Thallium contamination of desert soil in Namibia: chemical, mineralogical and isotopic insights. Environ. Pollut. 239, 272–280.

Howarth, S., Prytulak, J., Little, S.H., Hammond, S.J., Widdowson, M., 2018. Thallium concentration and thallium isotope composition of lateritic terrains. Geochim. Cosmochim. Acta, 239, 446–462.

Hou, D., O'Connor, D., Igalavithana, A.D., Alessi, D.S., Luo, J., Tsang, D.C.W., Sparks, D. L., Yamauchi, Y., Rinklebe, J., Ok, Y.S., 2020. Metal contamination and bioremediation of agricultural soils for food safety and sustainability. Nat. Rev. Earth Environ. 1, 366–381.

Jiang, Y., Wei, X., He, H., She, J., L, J., Fang, F., Zhang, W., Liu, Y., Wang, J., Xiao, T., Tsang, D.C.W., 2022. Transformation and fate of thallium and accompanying metal (loid)s in paddy soils and rice: a case study from a large-scale industrial area in China. J. Hazard. Mater. 423, 126997.

Karbowska, B., 2016. Presence of thallium in the environment: sources of contaminations, distribution and monitoring methods. Environ. Monit. Assess. 188, 640.

Kersten, M., Xiao, T., Kreissig, K., Brett, A., Coles, B.J., Rehkämper, M., 2014. Tracing anthropogenic thallium in soil using stable isotope compositions. Environ. Sci. Technol. 48 (16), 9030–9036.

Komárek, M., Ratié, G., Vaňková, Z., Šípková, A., Chrastný, V., 2021. Metal isotope complexation with environmentally relevant surfaces: Opening the isotope fractionation black box. Crit. Rev. Environ. Sci. Technol. https://doi.org/10.1080/10643389.2021.1955601.

Liu, J., Wang, J., Chen, Y., Xie, X., Qi, J., Lippold, H., Luo, D., Wang, C., Su, L., He, L., 2016. Thallium transformation and partitioning during Pb-Zn smelting and environmental implications. Environ. Pollut., 212, 77–89.

Liu, J., Han, G., 2021. Tracing riverine particulate black carbon sources in Xijiang River Basin: insight from stable isotopic composition and Bayesian mixing model. Water Res. 194, 116932.

Liu, J., Luo, X., Sun, Y., Tsang, D.C.W., Qi, J., Zhang, W., Li, N., Yin, M., Wang, J., Lippold, H., Chen, Y., Sheng, G., 2019. Thallium pollution in China and removal technologies for waters: a review. Environ. Int. 126, 771–790.

Liu, J., Yin, M., Xiao, T., Zhang, C., Tsang, D.C.W., Bao, Z., Zhou, Y., Chen, Y., Luo, X., Yuan, W., Wang, J., 2020. Thallium isotopic fractionation in industrial process of pyrite smelting and environmental implications. J. Hazard. Mater. 384, 121378. https://doi.org/10.1016/j.jhazmat.2019.121378.

Liu, J., Luo, X., Wang, J., Xiao, T., Chen, D., Sheng, G., Yin, M., Lippold, H., Wang, C., Chen, Y., 2017. Thallium contamination in arable soils and vegetables around a steel plant—a newly-found significant source of Tl pollution in south China. Environ. Pollut. 224, 445–453.

Liu, J., Ouyang, Qi'en, Wang, L., Wang, J., Zhang, Q., Wei, X., Lin, Y., Zhou, Y., Yuan, W., Xiao, T., 2022. Quantification of smelter-derived contributions to thallium contamination in river sediments: novel insights from thallium isotope evidence. J. Hazard. Mater. 424, 127594. https://doi.org/10.1016/j.jhazmat.2021.127594.

Liu, J., Zhang, J., Sun, G., Buyukada, M., Evrendilek, F., Dang, X., 2020. Thermodynamic equilibrium simulations of thallium distributions in interactions with chlorine, sulfur, phosphorus, and minerals during sludge co-combustion. Waste Biomass Valorizat. 11, 1251–1259.

Liu, J., Zhou, Y., She, J., Tsang, D., Lippold, H., Wang, J., Jiang, Y., Wei, X., Yuan, W., Luo, X., Zhai, S., Song, L., 2020. Quantitative isotopic fingerprinting of thallium associated with potentially toxic elements (PTEs) in fluvial sediment cores with multiple anthropogenic sources. Environ. Pollut. 266, 115252.

Martin, L.A., Wissocq, A., Benedetti, M.F., Latrille, C., 2018. Thallium (Tl) sorption onto illite and smectite: implications for Tl mobility in the environment. Geochim. Cosmochim. Acta 230, 1–16.

Maya-López, M., Mireles-García, M.V., Ramírez-Toledo, M., Colín-González, A.L., Galván-Arzate, S., Túnez, I., Santamaría, A., 2018. Thallium-induced toxicity in rat brain crude synaptosomal/Mitochondrial fractions is sensitive to anti-excitatory and antioxidant agents. Neurotox. Res. 33 (3), 634–640.

Migaszewski, Z.M., Gałuszka, A., 2021. Abundance and fate of thallium and its stable isotopes in the environment. Rev. Environ. Sci. Bio/Technol. 20 (1), 5–30.

Mirza, R., Moeinaddini, M., Pourebrahim, S., Zahed, M.A., 2019. Contamination, ecological risk and source identification of metals by multivariate analysis in surface sediments of the khouran straits, the Persian Gulf. Mar. Pollut. Bull. 145, 526–535.

Nielsen, S.G., Rehkämper, M., Baker, J., Halliday, A.N., 2004. The precise and accurate determination of thallium isotope compositions and concentrations for water samples by MC-ICPMS. Chem. Geol. 204 (1-2), 109–124.

Nielsen, S.G., Rehkämper, M., Porcelli, D., Andersson, P., Halliday, A.N., Swarzenski, P. W., Latkoczy, C., Günther, D., 2005. The thallium isotope composition of the upper continental crust and rivers-an investigation of the continental sources of dissolved marine thallium. Geochim. Cosmochim. Acta 69 (8), 2007–2019.

Nielsen, S.G., Gannoun, A., Marnham, C., Burton, K.W., Halliday, A.N., Hein, J.R., 2011. New age for ferromanganese crust 109D-C and implications for isotopic records of lead, neodymium, hafnium, and thallium in the Pliocene Indian Ocean. Paleoceanography 26 (2), n/a–n/a.

Nielsen, S.G., Rehkämper, M., 2012. Thallium isotopes and their application to problems in earth and environmental science. Handbook of Environmental Isotope Geochemistry.

Nielsen, S.G., Wasylenki, L.E., Rehkämper, M., Peacock, C.L., Xue, Z., Moon, E.M., 2013. Towards an understanding of thallium isotope fractionation during adsorption to manganese oxides. Geochim. Cosmochim. Acta 117, 252–265.

Nielsen, S.G., Prytulak, J., Blusztajn, J., Shu, Y., Auro, M., Regelous, M., Walker, J., 2017a. Thallium isotopes as tracers of recycled materials in subduction zones:

review and new data for lavas from Tonga-Kermadec and Central America. J. Volcanol. Geotherm. 339, 23–40.
Nielsen, S.G., Rehkämper, M., Prytulak, J., 2017b. Investigation and application of thallium isotope fractionation. Rev. Mineral. Geochem. 82 (1), 759–798.
Osorio-Rico, L., Santamaria, A., Galván-Arzate, S., 2017. Thallium toxicity: general issues, neurological symptoms, and neurotoxic mechanisms. Adv. Neurobiol. 18, 345–353.
Ostic, R.G., El-Badry, H.M., Kohman, T.P., 1969. Isotopic composition of meteoritic thallium. Earth Planet. Sci. Lett. 7 (1), 72–76.
Owens, J.D., Nielsen, S.G., Horner, T.J., Ostrander, C.M., Peterson, L.C., 2017. Thallium isotopic compositions of euxinic sediments as a proxy for global manganese-oxide burial. Geochem. Cosmochim. Acta 213, 291–307.
Peacock, C.L., Moon, E.M., 2012. Oxidative scavenging of thallium by birnessite: explanation for thallium enrichment and stable isotope fractionation in marine ferromanganese precipitates. Geochim. Cosmochim. Acta 84, 297–313.
Rader, S.T., Mazdab, F.K., Barton, M.D., 2018. Mineralogical thallium geochemistry and isotope variations from igneous, metamorphic, and metasomatic systems. Geochim. Cosmochim. Acta 243, 42–65.
Rehkämper, M., Halliday, A.N., 1999. The precise measurement of Tl isotopic compositions by MC- ICPMS: application to the analysis of geological materials and meteorites. Geochim. Cosmochim. Acta 63 (6), 935–944.
Rehkämper, M., Nielsen, S.G., 2004. The mass balance of dissolved thallium in the oceans. Mar. Chem. 85 (3-4), 125–139.
Rickwood, C.J., King, M., Huntsman-Mapila, P., 2015. Assessing the fate and toxicity of thallium I and thallium III to three aquatic organisms. Ecotoxicol. Environ. Saf. 115, 300–308.
Rinklebe, J., Shaheen, S.M., El-Naggar, A., Wang, H., Du Laing, G., Alessi, D.S., Sik Ok, Y., 2020. Redox-induced mobilization of Ag, Sb, Sn, and Tl in the dissolved, colloidal and solid phase of a biochar-treated and un-treated mining soil. Environ. Int. 140, 105754. https://doi.org/10.1016/j.envint.2020.105754.
Samantaray, S., Sanyal, P., 2022. Sources and fate of organic matter in a hypersaline lagoon: a study based on stable isotopes from the Pulicat lagoon, India. Sci. Total Environ. 807, 150617.
Schauble, E.A., 2007. Role of nuclear volume in driving equilibrium stable isotope fractionation of mercury, thallium, and other very heavy elements. Geochim. Cosmochim. Acta 71 (9), 2170–2189.
She, J., Liu, J., He, H., Zhang, Q., Liu, Y., Wang, J., Yin, M., Wang, L., Wei, X., Huang, Y., Chen, C., Lin, W., Chen, N., Xiao, T., 2022. Microbial response and adaption to thallium contamination in soil profiles. J. Hazard. Mater. 423, 127080.
Shen, D., Lu, Z., Zhong, J., Zhang, S., Ye, Q., Wang, W., Gan, J., 2021. Combination of high specific activity carbon-14 labeling and high resolution mass spectrometry to study pesticide metabolism in crops: metabolism of cycloxaprid in rice. Environ. Int. 157, 106879.
Sinicropi, M.S., Caruso, A., Capasso, A., Palladino, C., Panno, A., Saturnino, C., 2010. Heavy metals: toxicity and carcinogenicity. Pharmacologyonline 2010 (2), 329–333.
Sun, X., Fan, D., Liu, M., Tian, Y., Pang, Y., Liao, H., 2018. Source identification, geochemical normalization and influence factors of heavy metals in Yangtze River Estuary sediment. Environ. Pollut. 241, 938–949.
US EPA., 2017. Stable Isotope Mixing Models for Estimating Source Proportions (Retrieved from). United States Environmental Protection Agency.
USGS (US Geological Survey) (2019) Mineral Commodity. Summaries 2019.
Vaněk, A., Grösslová, Z., Mihaljevič, M., Trubač, J., Ettler, V., Teper, L., Cabala, J., Rohovec, J., Zádorová, T., Penížek, V., Pavlů, L., Holubík, O., Němeček, K., Houška, J., Drábek, O., Ash, C., 2016. Isotopic tracing of thallium contamination in soils affected by emissions from coal-fired power plants. Environ. Sci. Technol. 50 (18), 9864–9871.
Vaněk, A., Grösslová, Z., Mihaljevič, M., Ettler, V., Trubač, J., Chrastný, V., Penížek, V., Teper, L., Cabala, J., Voegelin, A., Zádorová, T., Oborná, V., Drábek, O., Holubík, O., Houška, J., Pavlů, L., Ash, C., 2018. Thallium isotopes in metallurgical wastes/contaminated soils: a novel tool to trace metal source and behavior. J. Hazard. Mater. 343, 78–85.
Vaněk, A., Holubík, O., Oborná, V., Mihaljevič, M., Trubač, J., Ettler, V., Pavlů, L., Vokurková, P., Penížek, V., Zádorová, T., Voegelin, A., 2019. Thallium stable isotope fractionation in white mustard: implications for metal transfers and incorporation in plants. J. Hazard. Mater. 369, 521–527.
Vaněk, A., Voegelin, A., Mihaljevič, M., Ettler, V., Trubač, J., Drahota, P., Vaňková, M., Oborná, V., Vejvodová, K., Penížek, V., Pavlů, L., Drábek, O., Vokurková, P., Zádorová, T., Holubík, O., 2020. Thallium stable isotope ratios in naturally Tl-rich soils. Geoderma 364, 114183. https://doi.org/10.1016/j.geoderma.2020.114183.
Vaněk, A., Vejvodová, K., Mihaljevič, M., Ettler, V., Trubač, J., Vaňková, M., Goliáš, V., Teper, L., Sutkowska, K., Vokurková, P., Penížek, V., Zádorová, T., Drábek, O., 2021. Thallium and lead variations in a contaminated peatland: a combined isotopic study from a mining/smelting area. Environ. Pollut. 290, 117973. https://doi.org/10.1016/j.envpol.2021.117973.
Viraraghavan, T., Srinivasan, A., 2011. Thallium: Environmental pollution and health effects. In Encyclopedia of Environmental Health, Elsevier: Burlington, pp, 325−333.
Vejvodová, K., Vaněk, A., Mihaljevič, M., Ettler, V., Trubač, J., Vaňková, M., Drahota, P., Vokurková, P., Penížek, V., Zádorová, T., Tejnecký, V., Pavlů, L., Drábek, O., 2020. Thallium isotopic fractionation in soil: the key controls. Environ. Pollut. 265, 114822.
Voegelin, A., Pfenninger, N., Petrikis, J., Majzlan, J., Plötze, M., Senn, A.-C., Mangold, S., Steininger, R., Göttlicher, J., 2015. Thallium speciation and extractability in a thallium- and arsenic-rich soil developed from mineralized carbonate rock. Environ. Sci. Technol. 49 (9), 5390–5398.
Wang, J., She, J., Zhou, Y., Tsang, D.C.W., Beiyuan, J., Xiao, T., Dong, X., Chen, Y., Liu, J., Yin, M., Wang, L., 2020. Microbial insights into the biogeochemical features of thallium occurrence: a case study from polluted river sediments. Sci. Total Environ. 739, 139957. https://doi.org/10.1016/j.scitotenv.2020.139957.
Walder, A.J., Freedman, P.A., 1992. Communication. Isotopic ratio measurement using a double focusing magnetic sector mass analyser with an inductively coupled plasma as an ion source. J. Anal. Atom. Spectr. 7 (3), 571. https://doi.org/10.1039/ja9920700571.
Wang, J., Wang, L., Wang, Y., Tsang, D., Yang, X., Beiyuan, J., Yin, M., Xiao, T., Jiang, Y., Lin, W., Zhou, Y., Liu, J., Wang, L., Zhao, M., 2021. Emerging risks of toxic metal (loid)s in soil-vegetables influenced by steel-making activities and isotopic source apportionment. Environ. Int. 146, 106207.
Wang, J., Yin, M., Liu, J., Shen, C.-C., Yu, T.-L., Li, H.-C., Zhong, Q., Sheng, G., Lin, K., Jiang, X., Dong, H., Liu, S., Xiao, T., 2021. Geochemical and U-Th isotopic insights on uranium enrichment in reservoir sediments. J. Hazard. Mater. 414, 125466.
Wang, J., Zhou, Y., Dong, X., Yin, M., Tsang, D., Sun, J., Liu, J., Song, G., Liu, Y., 2020. Temporal sedimentary record of thallium pollution in an urban lake: an emerging thallium pollution source from copper metallurgy. Chemosphere 242, 125172.
Wang, J.. Liu, S., Wei, X., Beiyuan, J., Wang, L., Liu, J., Sun, H., Zhang,G., Xiao, T., 2022. Uptake, organ distribution and health risk assessment of potentially toxic elements in crops in abandoned indigenous smelting region. Chemosphere, 292, 133321.
Wei, X., Zhou, Y., Jiang, Y., Tsang, D., Zhang, C., Liu, J., Zhou, Y., Yin, M., Wang, J., Shen, N., Xiao, T., Chen, Y., 2020. Health risks of metal(loid)s in maize (*Zea mays L.*) in an artisanal zinc smelting zone and source fingerprinting by lead isotope. Sci. Total Environ. 742, 140321.
Wei, X., Zhou, Y., Tsang, D., Song, L., Zhang, C., Yin, M., Liu, J., Xiao, T., Zhang, G., Wang, J., 2020. Hyperaccumulation and transport mechanism of thallium and arsenic in brake ferns (Pteris vittata L.): a case study from mining area. J. Hazard. Mater. 388, 121756.
Weiss, D.J., Rehkdmper, M., Schoenberg, R., McLaughlin, M., Kirby, J., Campbell, P.G.C., Arnold, T., Chapman, J., Peel, K., Gioia, A.S., 2008. Application of nontraditional stable isotope systems to the study of sources and fate of metals in the environment. Environ. Sci. Technol. 42 (3), 655–664.
Wick, S., Baeyens, B., Marques Fernandes, M., Voegelin, A., 2018. Thallium adsorption onto illite. Environ. Sci. Technol. 52 (2), 571–580.
Wick, S., Peña, J., Voegelin, A., 2019. Thallium sorption onto manganese oxides. Environm. Sci. Technol. 53 (22), 13168–13178.
Wick, S., Baeyens, B., Marques Fernandes, M., Göttlicher, J., Fischer, M., Pfenninger, N., Plötze, M., Voegelin, A., 2020. Thallium sorption and speciation in soils: role of micaceous clay minerals and manganese oxides. Geochim. Cosmochim. Acta 288, 83–100.
Wiederhold, J.G., 2015. Metal stable isotope signatures as tracers in environmental geochemistry. Environ. Sci. Technol. 49 (5), 2606–2624.
Wojtkowiak, T., Karbowska, B., Zembrzuski, W., Siepak, M., Lukaszewski, Z., 2016. Miocene colored waters: a new significant source of thallium in the environment. J. Geochem. Explor. 161, 42–48.
Xiao, J., Han, X.X., Sun, S.Q., Wang, L.Q., Rinklebe, J., 2021. Heavy metals in different moss species in alpine ecosystems of Mountain Gongga, China, geochemical characteristics and controlling factors. Environ. Pollut. 272, 115991.
Xiao, J., Lv, G.R., Chai, N.P., Hu, J., Jin, Z.D., 2022. Hydrochemistry and source apportionment of boron, sulfate, and nitrate in the Fen River, a typical loess covered area in the eastern Chinese Loess Plateau. Environ. Res. 206, 112570.
Yin, M., Sun, J., Chen, Y., Wang, J., Shang, J., Belshaw, N., Shen, C., Liu, J., Li, H., Linghu, W., Xiao, T., Dong, X., Song, G., Xiao, E., Chen, D., 2019. Mechanism of uranium release from uranium mill tailings under long-term exposure to simulated acid rain: geochemical evidence and environmental implication. Environ. Pollut. 244, 174–181.
Yin, M., Zhou, Y., Tsang, D., Beiyuan, J., Song, L., She, J., Wang, J., Zhu, L., Fang, F., Wang, L., Liu, J., Liu, Y., Song, G., Chen, D., Xiao, T., 2021. Emergent thallium exposure from uranium mill tailings. J. Hazard. Mater. 407, 124402.
Zeng, J., Han, G., 2020. Preliminary copper isotope study on particulate matter in Zhujiang River, Southwest China: application for source identification. Ecotoxicol. Environ. Saf. 198, 110663.
Zhang, Q., Rickaby, R.E.M., 2020. Interactions of thallium with marine phytoplankton. Geochim. Cosmochim. Acta 276, 1–13.
Zhong, Q., Yin, M., Zhang, Q., Beiyuan, J., Liu, J., Yang, X., Wang, J., Wang, L., Jiang, Y., Xiao, T., Zhang, Z., 2021. Cadmium isotopic fractionation in lead-zinc smelting process and signatures in fluvial sediments. J. Hazard. Mater. 411, 125015. https://doi.org/10.1016/j.jhazmat.2020.125015.
Zhong, Q., Zhou, Y., Tsang, D.C.W., Liu, J., Yang, X., Yin, M., Wu, S., Wang, J., Xiao, T., Zhang, Z., 2020. Cadmium isotopes as tracers in environmental studies: a review. Sci. Total Environ. 736, 139585. https://doi.org/10.1016/j.scitotenv.2020.139585.
Zhou, Y., He, H., Wang, J., Liu, J., Lippold, H., Bao, Z., Wang, L., Lin, Y., Fang, F.a., Huang, Y., Jiang, Y., Xiao, T., Yuan, W., Wei, X., Tsang, D.C.W., 2022. Stable isotope fractionation of thallium as novel evidence for its geochemical transfer during lead-zinc smelting activities. Sci. Total Environ. 803, 150036. https://doi.org/10.1016/j.scitotenv.2021.150036.
Zhou, Y., Wang, L., Xiao, T., Chen, Y., Beiyuan, J., She, J., Zhou, Y., Yin, M., Liu, J., Liu, Y., Wang, Y., Wang, J., 2020. Legacy of multiple heavy metal(loid)s contamination and ecological risks in farmland soils from a historical artisanal zinc smelting area. Sci. Total Environ. 720, 137541.
Zhuang, W., Liu, M., Song, J., Ying, S.C., 2021. Retention of thallium by natural minerals: a review. Sci. Total Environ. 777, 146074. https://doi.org/10.1016/j.scitotenv.2021.146074.